Aug 24th, 12:00 AM - Aug 25th, 12:00 AM

Mechanisms of Block Shear Failure of Bolted Connections

Lip H. Teh

Drew D. A. Clements

Twenty-First International Specialty Conference on Cold-Formed Steel Structures
St. Louis, Missouri, USA, October 24 & 25, 2012

Mechanisms of Block Shear Failure of Bolted Connections

Lip H. Teh[1] and Drew D. A. Clements[2]

Abstract

This paper examines the mechanisms for block shear failure postulated in the design provisions specified in the North American Specification for the Design of Cold-formed Steel Structural Members 2007 and AS/NZS 4600:2005 Cold-formed Steel Structures. It explains that there is only one feasible mechanism for the limit state of conventional block shear failure, that which involves shear yielding and tensile rupture. It proposes an equation that provides more accurate results compared to the code equations in predicting the block shear capacities of bolted connections in steels having minimal strain hardening. A resistance factor of 0.8 for the proposed equation is computed with respect to the LRFD approach given in the North American cold-formed steel specification.

Introduction

Block shear failure is recognised as a strength limit state of bolted connections in both the North American Specification for the Design of Cold-formed Steel Structural Members 2007 (AISI 2010) and AS/NZS 4600:2005 Cold-formed Steel Structures (SA/SNZ 2005). However, the pairs of design equations for block shear failure specified in the two codes are not exactly the same even though all the equations have been adopted from the AISC specifications (AISC 2010, 1993). The provisions against block shear failure of bolted connections in the AISC specifications (AISC 1978, 1986, 1993, 1999, 2010) have been evolving and even oscillating between certain equations, as described by Teh & Clements (2012).

[1]Senior Lecturer, School of Civil, Mining & Environmental Engineering, University Of Wollongong, Wollongong, NSW 2500, AUSTRALIA.
[2]Graduate Structural Engineer, Hatch, 25 Atchinson Street, Wollongong, NSW 2500, AUSTRALIA. Formerly Honours Student, School of Civil, Mining & Environmental Engineering, University Of Wollongong, Wollongong, NSW 2500, AUSTRALIA.

A major factor contributing to the repeated amendments is the uncertainty concerning the possible mechanisms for block shear failures. This paper discusses the mechanisms for block shear failure of bolted connections anticipated in the current cold-formed steel design codes.

Based on the mechanism identified as the only feasible one and the active shear resistance planes discussed in the companion paper (Clements & Teh 2012), this paper presents an equation for determining the block shear capacities of bolted connections in cold-formed steel sheets. The steel materials used in the experimental tests had low strain hardening, minimising the "noise" caused by shear strain hardening on the evaluation of alternative equations.

Current code equations for block shear failure strength

The nominal block shear failure strength of a bolted connection is specified in Clause E5.3 of the North American Specification for the Design of Cold-formed Steel Structural Members 2007 (AISI 2010) to be the lesser of the following

$$R_n = 0.6F_y A_{gv} + F_u A_{nt} \tag{1}$$

and

$$R_n = 0.6F_u A_{nv} + F_u A_{nt} \tag{2}$$

in which F_y is the yield stress, A_{gv} is the gross shear area, F_u is the tensile strength, A_{nt} is the net tensile area, and A_{nv} is the net shear area. The regions corresponding to these areas as defined by the code are shown in Figure 1.

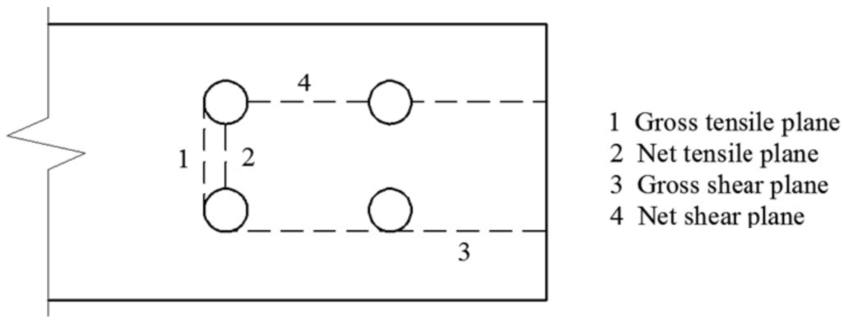

Figure 1 Gross and net shear planes

Equation (1) represents the block shear failure by shear yielding and tensile rupture, while Equation (2) postulates the simultaneous shear and tensile ruptures mechanism.

Clause 5.6.3 of AS/NZS 4600:2005 Cold-formed Steel Structures (SA/SNZ 2005) specifies the nominal block shear failure strength of a bolted connection to be

a) For $F_u A_{nt} \geq 0.6 F_u A_{nv}$: Equation (1)

b) For $F_u A_{nt} \leq 0.6 F_u A_{nv}$: $R_n = 0.6 F_u A_{nv} + F_y A_{gt}$ (3)

in which A_{gt} is the gross shear area corresponding to Region 1 in Figure 1. Equation (3) anticipates the shear rupture and tensile yielding mechanism.

Mechanisms for block shear failure of bolted connections

Consider the connected end of a flat member shown in Figure 2 that is subjected to a concentric load and is restrained from out-of-plane failure modes. Leaving out the pure net section tension failure mode and the bearing failure mode from the present discussion, there are essentially only two possible failure modes for the connected end. If the connection shear length (denoted by e_n in Figure 2) is relatively short, it will fail by "shear out" of each bolt, a distinct failure mode illustrated in Figure 3(a).

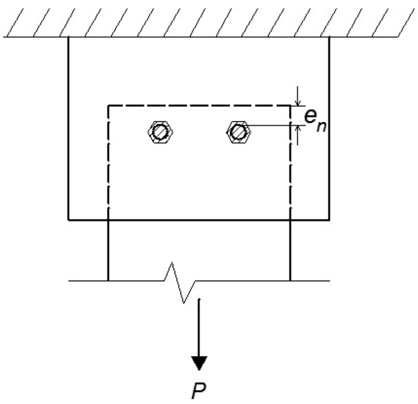

Figure 2 A two-bolt connection

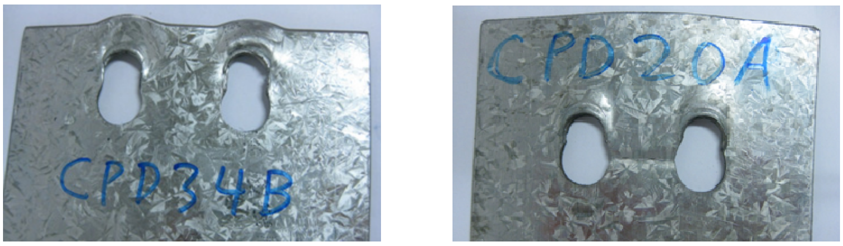

(a) Shear-out (b) Block shear failure

Figure 3 Two possible failure modes

Section E5.1 of Supplement No. 2 to the North American Specification for the Design of Cold-Formed Steel Structural Members (AISI 2010) specifies the shear out capacity P_{sop} of the two-bolt connection in Figure 2 to be

$$P_{sop} = 0.6F_u A_{nv} = 2.4F_u t e_n \tag{4}$$

in which t is the thickness of the sheet.

It could be imagined that as the connection shear length e_n increases, or as the bolt spacing decreases, or both, any of which results in an increase of the aspect ratio, a condition would be reached such that it is conceivable for the connected end to undergo block shear failure by simultaneous shear and tensile ruptures postulated in Equation (2). The aspect ratio at which the hypothetical mechanism of simultaneous shear and tensile ruptures could occur is termed the threshold ratio in the present work.

In reality, a conventional block shear failure by the simultaneous shear and tensile rupture mechanism postulated in Equation (2) is not feasible. Once yielding around the perimeter of the block takes place and the block displaces as a whole, the tensile strains in the net section between bolt holes increase much more rapidly than the shear strains as the former cannot be redistributed while the latter relax relative to the former (note the arching in Figure 3b) so that the block eventually fails by shear yielding and tensile rupture.

Even at an aspect ratio that is slightly lower than the threshold ratio, a block shear failure by shear yielding and tensile rupture is still possible as shown in Figure 4, where the shear-out deformations were over-run by the shear yielding and tensile rupture mechanism. The change-over in the failure mode took place when yielding started in the tensile net section between the two bolt holes, where tensile rupture eventually took place. Yielding of the tensile net section took place following shear strain hardening along the shear-out paths.

Figure 4 Shear-out deformations gave way to block shear failure

As the aspect ratio increases beyond the threshold ratio, block shear failure can only be due to shear yielding and tensile rupture since the tensile strains are always more critical than the shear strains. An example of such a failure mode is shown in Figure 3(b), where tensile rupture took place in the net section between the two bolt holes. This theoretical exposition is borne out by extensive experimental tests (Hardash & Bjorhovde 1985, Seleim & LaBoube 1996, Huns et al. 2006).

Obviously, at an aspect ratio that is sufficiently lower than the threshold ratio, the shear-out failure mode governs. There is therefore no aspect ratio at which a block shear failure occurs by the shear rupture and tensile yielding mechanism postulated in Equation (3).

The present exposition does not account for the situation in which bolt hole deformations are such that shear rupture could precede tensile rupture. However, for the specimens tested by Seleim & LaBoube (1996) in which the bearing failure took place before the block shear failure, the mechanism was still shear yielding and tensile rupture. In these cases, the strength limit state was actually bearing failure rather than block shear failure. (It was not possible for the bearing failures to have followed the block shear failures, but the opposite must have ensued when the tests were continued well past the ultimate bearing capacities, resulting in the reduction of the shear resistance area of each block.)

Proposed equation for block shear failure strength

The strength limit state of block shear failure

As explained in the preceding section, among the various mechanisms postulated in the literature for conventional block shear failures, there is only one feasible mechanism, that which involves shear yielding and tensile rupture. In this mechanism, as the block displaces, the tensile strains at the upstream net section increase with the applied load until necking occurs. With continuing displacements of the block, the tensile strains keep increasing but at one point the applied load has to decrease to maintain static equilibrium due to the necked tension area. The point at which the applied load has to decrease is the limit load identified in Figure 5. When the tensile strain adjacent to a bolt hole reaches the critical value, fracture propagates away from the bolt hole across the tensile net section, causing an abrupt drop in the resistance as shown in Figure 5 for a specimen tested in the present work.

It is possible for a connection with a very high aspect ratio in which the shear resistance dominates to undergo a second limit load following the tensile rupture that is higher than the first limit load. However, for the purpose of the present work, the block shear capacity of a bolted connection is defined as the maximum load preceding the tensile rupture, as represented by the limit load in Figure 5.

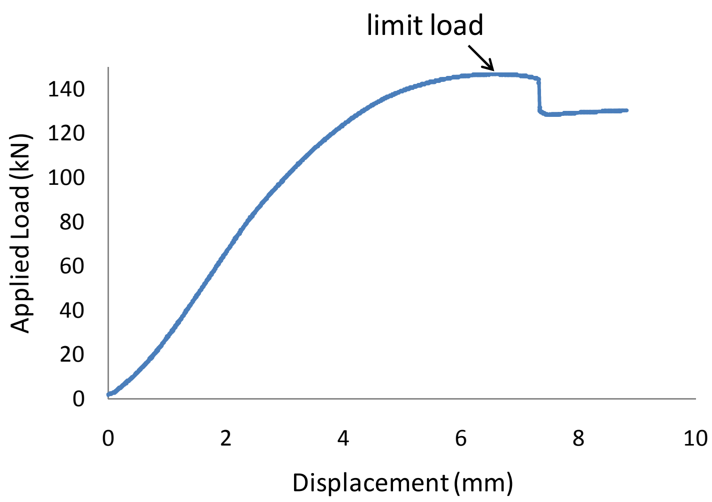

Figure 5 Definition of block shear capacity

Material and geometric properties for determining the block shear capacity

In the literature, evaluations of contesting equations for determining the block shear capacities of bolted connections have been somewhat clouded by two offsetting factors:

1. All specimens tested in the laboratories were composed of steel materials having high ratios of ultimate strength to yield stress (F_u/F_y), with a median ratio of greater than 1.55 for the specimens studied by Birkemoe & Gilmor (1978), Ricles & Yura (1983) and Hardash & Bjorhovde (1985). The lowest ratio was 1.30 (for one 6.4 mm thick cold-rolled steel specimen mistakenly used in the test program by Hardash & Bjorhovde 1985), and the highest was 1.75. The steel material recently used by Huns et al. (2006) had a ratio of 1.33. Since shear strain hardening may precede a block shear failure, the use of the yield stress in the evaluated equations for computing the shear yield resistance tends to underestimate its contribution.

2. Most evaluated equations use the gross area for computing the yield resistance component of a block shear capacity. Since in reality the gross area is not wholly available, such an approach tends to overestimate the yielding resistance.

As the two factors may offset each other, Equation (1) was often found to provide the most reasonable (albeit significantly varied) results compared to the other evaluated equations.

The authors note the experimental evidence of Franchuk et al. (2003), which suggests that the actual shear failure planes lie midway between the gross and the net shear planes indicated in Figure 1. The location of these so-called active shear planes, defined in Figure 6, has been confirmed through geometric and material nonlinear contact finite element analysis (Clements & Teh 2012).

For the sake of conservatism and simplicity, the present work uses the yield stress in determining the shear resistance component of the block shear capacity. For cold-reduced high-strength sheet steels including the G450 steel materials used in the present work, the ratio of ultimate tensile strength to yield stress can be significantly below 1.10.

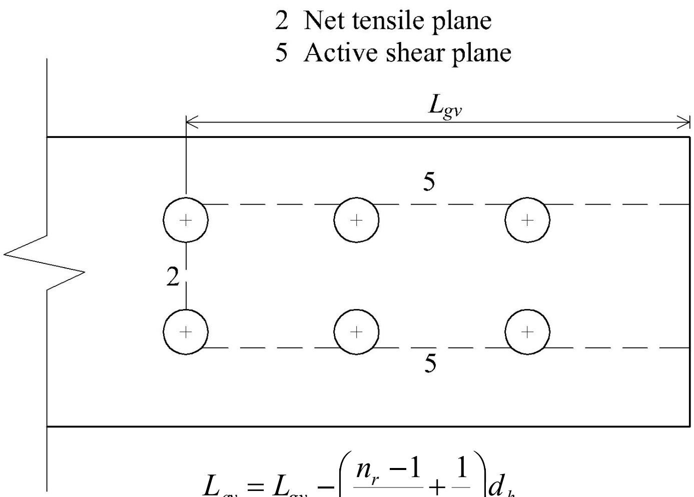

$$L_{av} = L_{gv} - \left(\frac{n_r - 1}{2} + \frac{1}{4}\right) d_h$$

$$\approx L_{gv} - {n_r d_h}/{2}$$

$$A_{av} = 2 L_{av} t$$

Figure 6 Tensile and shear resistance planes defined in the present work

The proposed equation

Based on the preceding expositions and the conclusion of Teh & Gilbert (2012) regarding the effect of in-plane shear lag on the tension capacity of a net section, the block shear failure strength of a bolted connection should be computed from

$$R_n = 0.6 F_y A_{av} + F_u \sum A_{nt} \left(0.9 + 0.1\, {d}/{p_2}\right) \tag{5}$$

in which the active shear area A_{av} is determined from the length of the active shear planes shown in Figure 6. The variable d denotes the bolt diameter and p_2 the bolt spacing in the tensile resistance plane, defined in Figure 7.

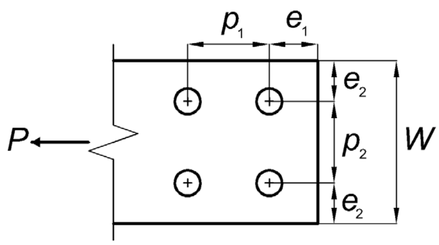

Figure 7 Geometric variables of a bolted connection

Equation (5) incorporates an in-plane "shear lag factor" proposed by Teh & Gilbert (2012) in determining the net section tension capacity. The shear lag factor accounts for the fact that the tensile stresses are not uniformly distributed across the net section, which has a significant effect on the tension capacity of bolted connections in cold-reduced sheet steel.

Test materials

Two nominal thicknesses were used in the present work, being 1.5 mm and 3.0 mm. The average base metal thicknesses t_{base}, yield stresses F_y, tensile strengths F_u and elongations at fracture over 15 mm, 25 mm and 50 mm gauge lengths ε_{15}, ε_{25} and ε_{50}, and uniform elongation outside fracture ε_{uo} of the steel materials as obtained from six 12.5 mm wide tension coupons are shown in Table 1. Tensile loadings of all coupons and bolted connection specimens are in the direction transverse to the rolling direction of the G450 sheet steel. The tension coupon tests were conducted at a constant stroke rate of 1 mm/minute resulting in a strain rate of about 2×10^{-4} per second prior to necking.

Table 1 Average material properties

	t_{base} (mm)	F_y (MPa)	F_u (MPa)	F_u / F_y	ε_{15} (%)	ε_{25} (%)	ε_{50} (%)	ε_{uo} (%)
1.5 mm	1.48	605	630	1.04	21.3	18.0	12.0	6.8
3.0 mm	2.95	530	580	1.09	29.3	22.0	15.3	8.1

The tensile strengths in the direction transverse to the rolling direction of 1.5 mm and 3.0 mm G450 sheet steels obtained in the present work, rounded to the nearest 5 MPa, are 6% and 10% higher than those obtained by Teh & Hancock

(2005) in the rolling direction. While Teh & Hancock (2005) did not provide the ratios of ultimate tensile strength to yield stress, it is believed that the transverse direction is associated with lower ratios. Any errors or offsetting effects arising from the neglect of strain hardening in Equation (5) are thus minimised.

Specimen configurations and test arrangements

Two connection series were tested to investigate the accuracy of the code and proposed equations in predicting the block shear capacities of simple bolted connections in 1.5 mm and 3.0 mm G450 sheet steels. Series A comprised connections having a single row of two bolts, and Series B connections having two such rows, as shown in Figure 8. For each series of a given sheet thickness, 12 mm and 16 mm bolts were used. The bolt holes were nominally 1 mm larger than the corresponding nominal bolt diameters. The bolts were only installed by hand with minimal tightening, and no washers were used in all the tests.

(a) Series A (b) Series B

Figure 8 Series A and B configurations

All specimens were subjected to concentric loading as illustrated in Figure 9 to exclude the effects of eccentric loading on the present study. The critical component is the inner sheet. For the purpose of ensuring that the connected sheets remained vertical throughout the tensile test, a shim plate of the same thickness as the sheet was welded to one of the outer sheets.

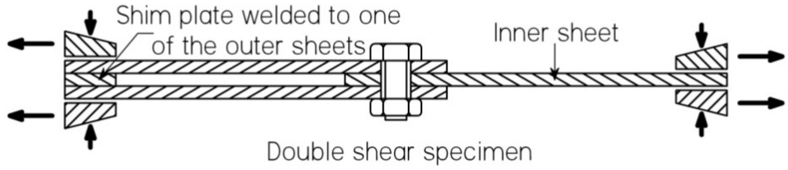

Figure 9 Concentric loading of critical component

Experimental test results and discussions

In calculating the block shear capacity R_n of a specimen predicted by design equations, the measured values of the geometric dimensions such as the base metal thickness, the bolt hole diameter and the bolt spacing were used. However, for ease of comparisons, only the nominal values are shown in the tables following.

Table 2 lists the relevant geometric dimensions and the test results of Series A specimens (see Figure 8a for an example) which underwent the block shear failure mode. All of them duly failed by the shear yielding and tensile rupture mechanism. The variable d_h denotes the nominal bolt hole diameter. Other variables are defined in Figure 7.

Table 2 shows the ratios of the ultimate test load P_t to the block shear failure strength R_n predicted by Equations (1), (2), (3) and (5). The first three are code equations, while the last is proposed in the present work. As explained in the preceding sections, Equations (2) and (3) do not represent the true mechanism of block shear failures.

It can be seen from Table 2 that Equation (1), which is used in both cold-formed steel design codes (AISI 2010, SA/SNZ 2005) for determining the block shear failure load due to the shear yielding and tensile rupture mechanism, consistently and significantly overestimates the block shear capacities of Series A specimens.

Equation (3), which postulates the mechanism of shear rupture and tensile yielding, overestimates the capacity of some specimens by almost 40%. Equation (2), on the other hand, overestimates the block shear capacities by up to 10% “only”. However, it should be noted that this equation postulates the incorrect mechanism of simultaneous shear and tensile ruptures, while all the specimens failed by the shear yielding and tensile rupture mechanism.

Table 2 Results of Series A specimens

Spec	W (mm)	p_2 (mm)	t (mm)	e_1 (mm)	d_h (mm)	P_t/R_n			
						(1)	(2)	(3)	(5)
CPD14	100	33	1.5	50	17	0.80	0.90	0.72	0.95
CPD15	100	33	3.0	50	13	0.90	0.93	0.82	1.01
CPD16	100	33	3.0	50	17	0.89	0.96	0.79	1.04
CPD18	120	40	1.5	50	17	0.86	0.96	0.79	1.00
CPD19	120	40	3.0	50	13	0.90	0.93	0.83	1.01
CPD20a	120	40	3.0	50	17	0.93	0.99	0.84	1.07
CPD20b	120	40	3.0	50	17	0.93	0.98	0.84	1.07
CPD22a	100	26	1.5	50	17	0.81	0.93	0.72	0.96
CPD22b	100	26	1.5	50	17	0.83	0.95	0.74	0.99
CPD23a	100	26	3.0	50	13	0.90	0.93	0.80	1.01
CPD23b	100	26	3.0	50	13	0.89	0.93	0.80	1.01
CPD24a	100	26	3.0	50	17	0.87	0.94	0.76	1.02
CPD24b	100	26	3.0	50	17	0.87	0.94	0.76	1.02
CPD26a	120	26	1.5	50	17	0.85	0.97	0.76	1.01
CPD26b	120	26	1.5	50	17	0.84	0.96	0.75	1.00
CPD27	120	26	3.0	50	13	0.91	0.94	0.81	1.02
CPD28a	120	26	3.0	50	17	0.91	0.98	0.79	1.06
CPD28b	120	26	3.0	50	17	0.89	0.96	0.77	1.04
CPD36	130	45	3.0	30	17	0.94	1.05	0.86	1.13
					$(P_t/R_n)_{av}$	0.88	0.95	0.79	1.02

Table 3 shows the outcomes for Series B specimens (see Figure 8b for an example) which underwent the block shear failure mode. All of them duly failed by the shear yielding and tensile rupture mechanism.

Table 3 Results of Series B specimens (p_1 = 30 mm)

Spec	***W* (mm)**	**p_2 (mm)**	***t* (mm)**	**e_1 (mm)**	**d_h (mm)**	**P_t/R_n**			
						(1)	**(2)**	**(3)**	**(5)**
CQ2a	120	26	1.5	50	17	0.73	1.01	0.82	0.92
CQ2b	120	26	1.5	50	17	0.74	1.02	0.84	0.93
CQ3	120	26	3.0	50	13	0.85	1.00	0.89	1.00
CQ4	120	26	3.0	50	17	0.80	1.02	0.86	0.99
CQ5a	130	40	1.5	30	13	0.82	1.04	0.91	0.99
CQ5b	130	40	1.5	30	13	0.81	1.02	0.89	0.98
CQ6a	130	40	1.5	30	17	0.77	1.08	0.88	0.98
CQ6b	130	40	1.5	30	17	0.77	1.09	0.88	0.99
CQ7	130	40	3.0	30	13	0.89	1.07	0.96	1.07
CQ8	130	40	3.0	30	17	0.83	1.13	0.94	1.06
CQ9b	130	55	1.5	30	13	0.81	1.00	0.89	0.97
CQ10a	130	55	1.5	30	17	0.78	1.04	0.89	0.98
CQ10b	130	55	1.5	30	17	0.80	1.06	0.90	1.00
CQ11	130	55	3.0	30	13	0.87	1.02	0.94	1.03
CQ12	130	55	3.0	30	17	0.85	1.10	0.96	1.06
					$(P_t/R_n)_{av}$	0.81	1.05	0.90	1.00

As is the case with Series A specimens, Equations (1) and (3) consistently and significantly overestimates the block shear capacities of Series B specimens. The major reason is the use of the gross area in computing the tensile or shear yielding resistance component of the block shear capacity. This effect is likely to have been hidden to various extent in the experimental tests of bolted connections in hot-rolled steel plates by considerable strain hardening due to the very high ratios of ultimate tensile strength to yield stress (F_u/F_y). In certain cases, it might have also been hidden by the much higher strain rates incurred during the bolted connection tests compared to the tension coupon tests, or by the bolt friction resistance.

Equation (2), which postulates the simultaneous shear and tensile rupture mechanism, predicts lower capacities for Series B specimens compared to the proposed Equation (5) despite its use of the tensile strength F_u rather than the yield stress F_y in computing the shear resistance. The conservatism is due to the over-reduced shear area A_{nv}, the effect of which increases with increasing number of bolt rows as the difference between the net and the active shear areas widens while the shear resistance becomes more important relative to the tensile resistance.

Equation (5), in conjunction with the active resistance planes defined in Figure 6, predicts the block shear capacities of Series A and B specimens with the greatest accuracy. It was found that in order to achieve or exceed the target reliability index β_0 of 3.5 in the LRFD, a resistance factor of 0.83 is required.

Conclusions

Among the various mechanisms for conventional block shear failures anticipated in the cold-formed steel design codes, there is only one feasible mechanism, that which involves shear yielding and tensile rupture.

The shear yielding and tensile rupture mechanism is represented by one equation common to the North American and the Australasian cold-formed steel design codes. This equation uses the gross shear area in determining the shear resistance to block shear failure, and therefore overestimates the block shear capacities of all specimens tested in the present work.

The other equation in the North American specification, which anticipates the simultaneous shear and tensile rupture mechanism, overestimates the block shear capacities of the single-row bolted connections, but underestimates those of the double-row bolted ones.

The other equation in the Australasian standard, which anticipates the shear rupture and tensile yielding mechanism, overestimates the block shear capacities of all specimens tested in the present work.

The equation proposed in this paper, which is based on the shear yielding and tensile rupture mechanism, and which uses the active shear resistance planes that lie midway between the gross and the net shear planes, and incorporates an in-plane shear lag factor, has been demonstrated to provide the most consistent and accurate results in predicting the block shear capacities of the tested specimens.

It is proposed that a resistance factor of 0.8 be applied to the new equation in order to ensure a reliability index of not less than 3.5 in the LRFD approach of the North American specification for the design of cold-formed steel structures.

References

AISC (1978) *Specification for the Design, Fabrication and Erection of Structural Steel for Buildings*, American Institute of Steel Construction, Chicago IL.

AISC (1986, 1993, 1999) *Load and Resistance Factor Design Specification for Structural Steel Buildings*, American Institute of Steel Construction, Chicago IL.

AISC (2010) *Specification for Structural Steel Buildings*, ANSI/AISC 360-10, American Institute of Steel Construction, Chicago IL.

AISI (2010) *Supplement No. 2 to the North American Specification for the Design of Cold-formed Steel Structural Members 2007 Edition*, American Iron and Steel Institute, Washington DC.

Birkemoe, P.C., and Gilmor, M.I. (1978) "Behavior of bearing-critical double-angle beam connections." *Engineering Journal AISC*, 15 (4), 109–115.

Clements, D. D. A., and Teh, L. H. (2012) "Active shear planes in block shear failure of bolted connections," presented in this conference.

Franchuk, C. R., Driver, R. G., and Grondin, G. Y. (2003) "Experimental investigation of block shear failure in coped steel beams." *Can. J. Civ. Eng.*, 30, 871-881.

Hardash, S. G., and Bjorhovde, R. (1985) "New design criteria for gusset plates in tension." *Engineering Journal AISC*, 22 (2), 77-94.

Huns, B. B. S., Grondin, G. Y., and Driver, R. G. (2006) "Tension and shear block failure of bolted gusset plates." *Can. J. Civil Engrg.*, 33, 395-408.

Ricles, J. M., and Yura, J. A. (1983) "Strength of double-row bolted web connections." *J. Struct. Div. ASCE*, 109 (ST1), 126-142.

SA/SNZ (2005) *Cold-Formed Steel Structures*, AS/NZS 4600:2005, Standards Australia/Standards New Zealand.

Seleim, S., and LaBoube, R.A. (1996) "Behavior of low ductility steels in cold-formed steel connections." *Thin-Walled Structures*, 25 (2), 135-150.

Teh, L. H., and Clements, D. D. A. (2012) "Block shear capacity of bolted connections in cold-reduced steel sheets," scheduled for publication in April 2012 in *J. Struct. Eng*., ASCE.

Teh, L. H., and Gilbert, B. P. (2012) "Net section tension capacity of bolted connections in cold-reduced steel sheets," *J. Struct. Eng.*, 138 (3), 337-344.

Teh, L. H., and Hancock, G. J. (2005) "Strength of welded connections in G450 sheet steels." *J. Struct. Eng.*, 131 (10), 1561-1569.